Journal of Materials Processing Technology 212 (2012) 27–35

Contents lists available at ScienceDirect

Journal of Materials Processing Technology

journal homepage: www.elsevier.com/locate/jmatprotec

Modeling and evaluation of curved layer fused deposition

Sarat Singamneni[a,*], Asimava Roychoudhury[b], Olaf Diegel[a], Bin Huang[a]

[a] School of Engineering, AUT University, Auckland, New Zealand
[b] Department of Mechanical Engineering, Indian Institute of Technology, Kharagpur, India

ARTICLE INFO

Article history:
Received 20 December 2010
Received in revised form 29 July 2011
Accepted 3 August 2011
Available online 9 August 2011

Keywords:
Rapid prototyping
Fused deposition modeling
Flat and curved layer slicing

ABSTRACT

Fused deposition modeling (FDM), one of the rapid prototyping techniques is a promising technology for rapid manufacture of end use parts direct from CAD files and with the proliferation of cheaper machines, is likely to play a vital role in future polymer processing, challenging traditional processes such as injection moulding in some cases. Research evidence suggests that the road and layer structures would have significant influences on the mesostructure and consequent mechanical behaviour of the resulting polymer part. While adaptive slicing and other deposition schemes have been attempted for different reasons, it is believed that an appropriate deposition scheme is essential to ensure the best inter-road and interlayer connectivity, resulting in a continuous network of polymer chains, as in the case of the traditional processes. The current research proposes the curved layer deposition for FDM, in particular for thin shell-like parts, to ensure fibre continuity. Mathematical models are developed for curved slicing, implemented in a few case studies, parts are printed, and test results suggest marked improvement in the mechanical characteristics of curved layer parts.

1. Introduction

In fused deposition modeling (FDM), parts are fabricated by extruding a semi-molten filament through a heated nozzle in a prescribed pattern onto a platform. The thermal energy associated with the semi-molten material drives the bonding and as the material is deposited, it bonds with the surrounding material, cools and solidifies (Bellehumeur et al., 2004). The end result is that FDM parts are orthotropic composites of partially bonded polymer filaments and voids. Two successive roads are bound by a sintering process, the first step of which is the establishment of interfacial molecular contact by wetting, followed by molecular motions towards preferred configurations to achieve the absorptive equilibrium. Molecules either diffuse or form chemical bonds across the interface and randomisation can only be achieved through extensive inter-diffusion of chain segments under critical conditions, while the size of the neck indicates the quality of the bonding.

The major controlling factor for the mechanical properties of FDM parts is the mesostructure, which can be altered by the adjustable fabrication parameters. While investigating with unidirectional P400 ABS plastic material parts built with FDM 1600 machine, Rodriguez et al. (2000) quantified the nature and range of the mesostructural tailoring capability of the FDM materials, clearly elucidating the need for further research aimed at process improvements. Further experimental evaluation of the influence of the mesostructure on mechanical properties showed significant mesostructural influence on the stress–strain response (Rodriguez et al., 2001). While elastic and shear moduli values 11–37 per cent lower and yield strength values 22–57 per cent lower than the ABS monofilament were noted, the same will also fall short of the injection moulded counterparts, and the build style and road structure would have significant influences on the final part characteristics.

Apart from the porous internal materials structure, the external surfaces are affected by stair-step effects resulting from the stacking of flat layers and the part orientation. This becomes more obvious on curved surfaces and particularly when using thicker layers. In order to build the part more accurately, the number of layers needs to be increased, by reducing the thickness of the flat layers (Sabourin et al., 1996) often leading to unacceptable build times. Adhesive strength between layers or across filaments is weaker than the strength of continuous filaments (Lee et al., 2007) and the air gap and raster orientation affect the tensile strength of FDM parts dramatically. While layer thickness, road width and speed by far remain the most significant parameters influencing the form and surface quality of prototypes (Anitha et al., 2001), in some specific cases, for example, the thin shell components, discontinuous filament structure deteriorates the part strength even further.

Analysis of structural quality of FDM parts made using metal and ceramic powders (Agarwala et al., 1996) and fused deposition of ceramics (Allahverdi et al., 2001) for a variety of ceramic

* Corresponding author at: Department of Mechanical and Manufacturing Engineering, School of Engineering, AUT University, 24 St. Paul's Street, Auckland 1020, New Zealand. Tel.: +64 09 921 9999 8002.
E-mail address: sarat.singamneni@aut.ac.nz (S. Singamneni).

0924-0136/$ – see front matter © 2011 Elsevier B.V. All rights reserved.
doi:10.1016/j.jmatprotec.2011.08.001

compounds are a couple of early attempts aimed at enhancing the FDM capabilities. Build direction effective from either the orientation of the deposition head (Xu et al., 1999) or the part orientation itself (Hu et al., 2002) could have significant influences on the part properties and build times. Slicing algorithms also significantly influence the part quality and build times and the following are some prominent attempts in this direction; Jamieson and Hacker (1995) attempted direct slicing of CAD models and observed enhanced dimensional accuracy and reduced processing times. While Kulkarni and Dutta (1996) implemented adaptive slicing based on variable thickness slicing for optimum number of slices and cusp-height, Sabourin et al. (1996) used stepwise uniform refinement, resulting in reduced build time, without losing the overall accuracy. Hope et al. (1997) developed an adaptive slicing procedure based on surface curvature and angle of the surface normal for the best geometric accuracy. Luo et al. (1999) proposed an efficient 3D slicing considering both the part and support structures.

Though some of these approaches led to subsequent improvements, there are further shortcomings, and the hypothesis for the current research is that in the case of thin shell-like parts such as the one shown in Fig. 1(a), curved layer slicing and deposition as shown in Fig. 1(c) result in better material structure and consequent part strength, due to fibre continuity, as against the conventional flat layer deposition as shown in Fig. 1(b). The experimental and simulation analyses of Yang et al. (2002) through equidistant path generation showed significant improvements in both process efficiency and part quality and one of the immediate effects of curved layer fused deposition modeling (CLFDM) is to achieve better placement of adjacent filaments.

Klosterman et al. (1999) developed a curved layer process based on laminated object manufacturing (LOM) technology for efficient production of curved layer parts. Monolithic ceramic (SiC) and CMC (SiC/SiC) articles were fabricated using Curved Layer Laminated Object Manufacturing (CLLOM). For making thin shell-type objects, the CLLOM process allowed advantages of eliminated stair step effect, increased building speed, reduced waste, and maintenance of continuous fibres in the direction of curvature. The current research aims at extending this to FDM, but, the raw material forms and process steps being different, a complete new set of algorithms and implementation schemes need development, before practically testing the effectiveness of curved layer FDM.

Chakraborty et al. (2008) developed a curved layer fused deposition modeling (CLFDM) algorithm which was formulated and tested on parametric surfaces. The mathematical models suggested were mainly theoretical and were never implemented in reality. The current research takes off from this point and delves into developing algorithms for curved layer slicing, practical implementation of the same for CLFDM, and subsequent testing of parts produced. While improvements such as better surface and part quality and reduced build times are expected to enhance the process capabilities of FDM in general, some future predictions are that these methods could also be of use in applications such as 3D printing of conductive polymers as envisioned by the current authors together with some other colleagues and collaborators (Diegel et al., 2011a,b). Different schemes for curved layer slicing are discussed in Sections 2–4 and the best combination of these is finally used for the case studies reported in Section 5 and the practical implementation and comparative assessment of flat and curved layer FDM parts discussed in Sections 6 and 7.

2. Generation of surface point data

The first step towards the curved layer slicing is modeling the top surface of the part for a given print orientation, to generate the surface point data. Subsequently, the offsetting algorithm uses this point cloud data to generate curved layers. Obviously, the geometrical quality of offset layers depends on the accuracy of the initial point cloud data. Two different methods are attempted in this research to generate the initial surface point data; one is through G&M code processing in a Computer Aided Manufacturing (CAM) module of any solid modeling software and the other is through processing an STL format file.

The G and M code method involves first creating the solid model of the object using one of the solid modelers, and subsequent processing of the same using the constituent CAM module, such as the Solid CAM or the manufacturing Module in UGNX. The CAM software generates the G&M codes automatically by following the shape of the top surface of the part with its own or user defined patterns, mostly in the zigzag format. In order to replicate the motions of the deposition nozzle when run on the RP machine, the G&M codes for the cutter path data are generated based on the three-axis milling with a ball end cutter of size equal to the diameter of the nozzle of the deposition head. Fig. 2 shows the basic shape of a thin curved part to be used for testing the proposed curved layer slicing and the cutter paths developed for the top surface, using the G and M code data generated by the Manufacturing Module in UGNX. The output from the CAM module is usually a text file containing the coordinates of surface points together with a lot of other information. A MATLAB program is written to retrieve the coordinate data from these files and ordering the data points in a sequence as to produce the deposition pathways for curved layer FDM as shown in Fig. 2(b).

The STL file is the de facto standard file format for RP currently and gathering the surface point data from STL files is another option for the CLFDM process. A STL file model, as shown in Fig. 3 can be created by any 3D engineering solid modeling software. As these files are in the binary form, it is hard to gather the point cloud data, and an open source MATLAB program, written by Harlev (2005), is used to collect the coordinates of the vertex points of surface triangles. The output is in the form of four matrices containing X, Y, and Z coordinates, and the colour of each facet. This data is further processed in MATLAB and after all coordinates of the vertices are located and saved in matrices, selected vertical planes are used to slice the STL model as shown in Fig. 4, to generate the necessary surface points.

Both methods are equally good as a starting point for the creation of the critical surface points of a given relatively simple shape. However, the STL file route is a more fundamental approach and allows a greater amount of freedom as the use of commercial CAD packages and associated standardization is eliminated. STL files are also amenable to further modification and optimisation through mesh refinement techniques, which is necessary to be able to explicitly identify top surfaces of objects of more complex shapes, as may be required in future when the curved layer approach will be applied in more practical cases. In fact, the direct slicing of CAD files based on the mathematical representation of surface data is the most ideal approach, and will be considered, once the specific attributes of CLFDM are established. In the current research, both G and M-code and STL file routes are successfully tested for initial trials and the G and M code method is finally employed for all the case studies and test pieces reported here.

3. Curved layer slicing

Generation of parallel curved slices has been attempted by different means, initially by offsetting all the points in the Z-direction by an amount equal to the thickness of the curved layer and then by considering the cross product of two vectors at every surface point. Though simple to use, both these methods suffer from drawbacks.

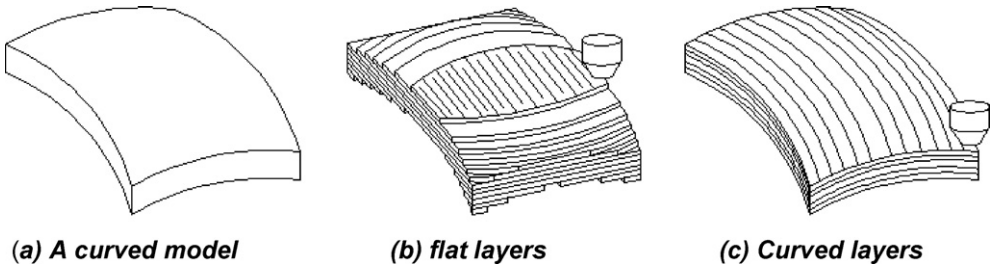

Fig. 1. Curved layer fused deposition modeling (CLFDM). (a) A curved model; (b) flat layers; (c) curved layers.

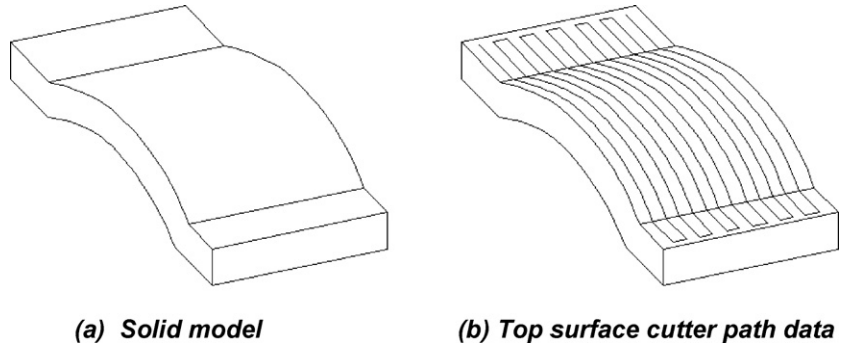

Fig. 2. Solid model of the test part and cutter path data. (a) Solid model; (b) top surface cutter path data.

While the *Z*-offsetting leads to distortion in shape in successive iterations and possible interference in deposition path lines, the latter method lacks precession to capture local variations in surface profiles and fails specifically at sharp edges and corners.

Alternatively, four vectors at each surface point, considering the four neighbouring points to construct the cross product vectors allow a better representation of surface variations. The vector construction scheme is shown in Fig. 5 and the constituent relationships for calculating the offset points are as follows:

$$\alpha_1 = a\cos\frac{\vec{V}_{13}\cdot\vec{V}_{14}}{|\vec{V}_{13}|\cdot|\vec{V}_{14}|}$$

$$\vec{V}_{13,14} = \frac{t}{\cos(\alpha_1/2)}\cdot\frac{\vec{V}_{13}\cdot\vec{V}_{14}}{|\vec{V}_{13}+\vec{V}_{14}|}$$

$$\alpha_2 = a\cos\frac{\vec{V}_{23}\cdot\vec{V}_{24}}{|\vec{V}_{23}|\cdot|\vec{V}_{24}|}$$

$$\vec{V}_{23,24} = \frac{t}{\cos(\alpha_2/2)}\cdot\frac{\vec{V}_{23}\cdot\vec{V}_{24}}{|\vec{V}_{23}+\vec{V}_{24}|}$$

$$\beta = a\cos\frac{\vec{V}_{13,14}\cdot\vec{V}_{23,24}}{|\vec{V}_{13,14}|\cdot|\vec{V}_{23,24}|}$$

$$\vec{V}_5 = \frac{t}{\cos(\alpha_1/2)\cos(\beta/2)}\cdot\frac{\vec{V}_{13,14}+\vec{V}_{23,24}}{|\vec{V}_{13,14}+\vec{V}_{23,24}|}$$

$$\vec{P}_{i,j,k+1} = \vec{P}_{i,j,k} + \vec{V}_5$$

where t is the thickness of the curved layer, $P_{i,j,k}$ and $P_{i,j,k+1}$ are the points on a given layer and the offset layer respectively, and V_{13}, V_{14}, etc. are vectors constructed.

$P_{i,j,k+1}$ is the new point on the offset curved layer. Though effective in capturing true surface variations, the method involves too many calculations and gets computationally intensive and is also

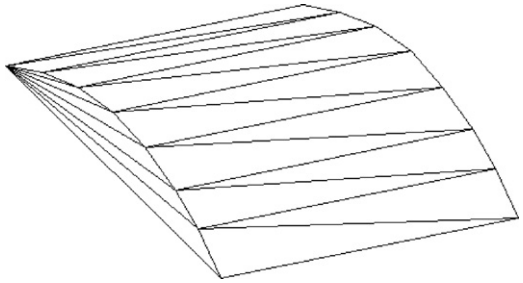

Fig. 3. Standard STL file.

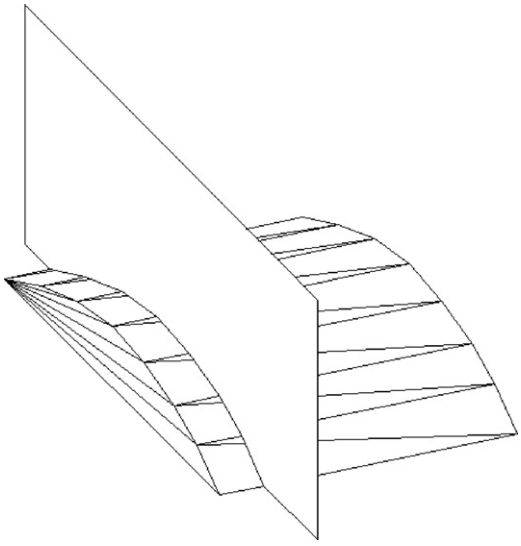

Fig. 4. Slicing triangulated objects.

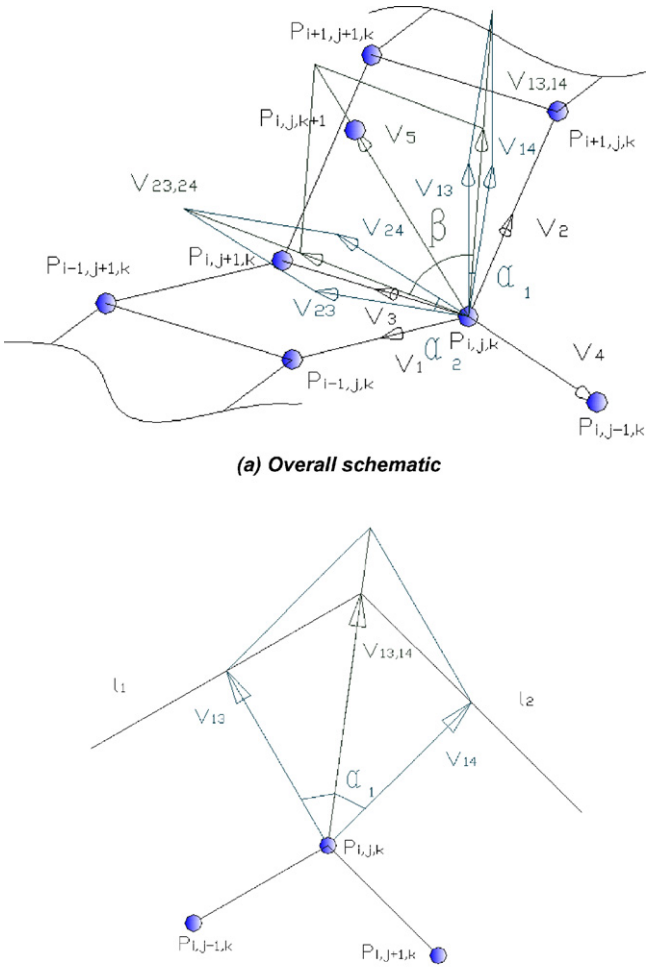

Fig. 5. The four vector method. (a) Overall schematic; (b) schematic of $V_{13,14}$.

sensitive to relative positioning of adjacent points. Further, the absence of surrounding points on all edges would require creation of external pseudo nodes, adding further calculations.

These issues are resolved by slightly modifying the four vector method considering a vertical plane passing through three consecutive surface points. This will work effectively in particular when the original surface points are generated by considering intersection of a series of parallel vertical planes with the model surface which is the case when using the STL files. The modified slicing process as shown in Fig. 6 employs two vectors on the surface and one auxiliary vector to construct the cross product vector. Once the surface point data is loaded, the slicing algorithm begins by creating two vectors V_1 and V_2 between points $P_{i,j,k}$, $P_{i-1,j,k}$ and $P_{i,j,k}$, $P_{i+1,j,k}$, respectively, while the auxiliary vector V_3 is perpendicular to the vertical plane J from $P_{i,j,k}$.

$$\vec{V}_1 = \vec{P}_{i-1,j,k} - \vec{P}_{i,j,k}$$

$$\vec{V}_2 = \vec{P}_{i+1,j,k} - \vec{P}_{i,j,k}$$

Two cross product vectors V_{13} and V_{23} are constructed following the right-hand rule based on vectors V_1, V_3 and V_2, V_3, respectively. The magnitudes of all the cross product vectors are equal to the thickness of the curved layer

$$\vec{V}_{13} = t \cdot \frac{\vec{V}_1 \times \vec{V}_3}{|\vec{V}_1 \times \vec{V}_3|}$$

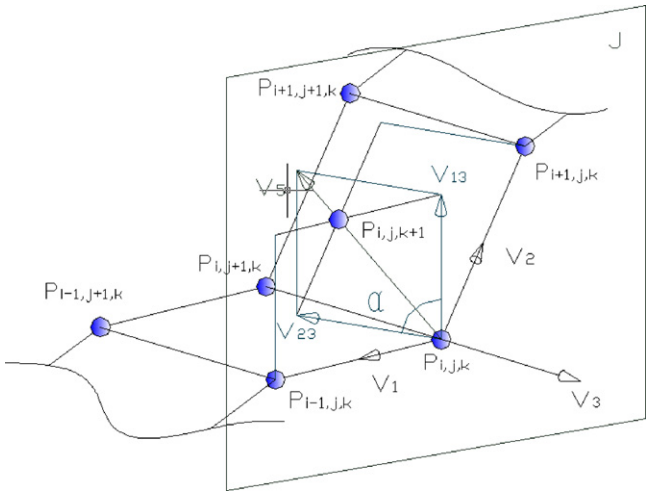

Fig. 6. The modified approach considering nodes on vertical planes.

$$\vec{V}_{23} = t \cdot \frac{\vec{V}_3 \times \vec{V}_2}{|\vec{V}_2 \times \vec{V}_3|}$$

The angle between these two vectors and the resulting vector V_5 are obtained using the following equations

$$\alpha = a\cos \frac{\vec{V}_{13} + \vec{V}_{23}}{|\vec{V}_{13}| \cdot |\vec{V}_{23}|}$$

$$\vec{V}_5 = \frac{t}{\cos(\alpha/2)} \frac{\vec{V}_{12} + \vec{V}_{23}}{|\vec{V}_{13} + \vec{V}_{23}|}$$

The end point of this vector is the target offset point on the curved layer and the new offset point is generated by

$$\vec{P}_{i,j,k+1} = \vec{P}_{i,j,k} + \vec{V}_5$$

A repetition of this on all points on a given surface and all successive surfaces would generate the point cloud data for each curved slice, which can be used for constructing the deposition path ways that will eventually be put together as a continuous line of deposition for the practical implementation of the scheme on a test facility. The modified method reduces the calculation time for curved slicing and proved to be less sensitive to local variations in surface points. It is also more independent and works even in cases where some data points are missing. This modified method based on consecutive points considered on parallel vertical planes is used for the curved layer slicing of all case studies and test parts analysed in this paper subsequently.

4. Support structures

For most curved parts, a support structure is usually needed, the shape of which depends on the part geometry. The current approach is to build the support structure using flat layers, as it is more convenient, without actually loosing much on quality. The deposition path data for the flat layer support structure can be developed by using one of the existing software packages of different FDM machines. However, it is practically difficult to integrate such data with the deposition systems used in the current research. As a result, an explicit scheme is devised for developing the deposition path data to build the support structures in flat layers. The bottom most curved layer is sliced with a number of horizontal and vertical planes, to obtain the set of points used to describe the deposition pathways for the flat layered support structure.

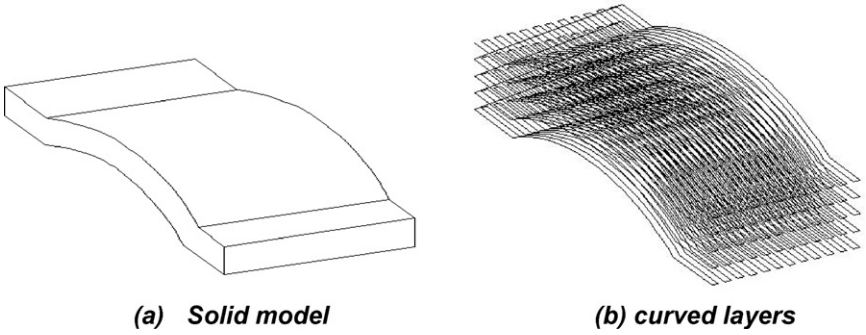

Fig. 7. The simple curved part. (a) Solid model; (b) curved layers.

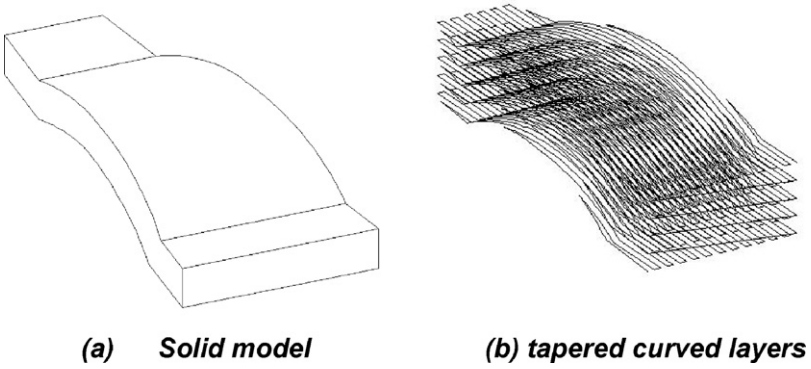

Fig. 8. A thin curved and tapered part. (a) Solid model; (b) tapered curved layers.

5. Case studies

Several case studies are then considered to test the final solutions developed for the curved layer slicing. Considering the example part shown in Fig. 2(a), the top surface data generated using the G and M code approach is processed using the modified vector method and curved layers parallel to the top surface and the deposition path patterns are generated as shown in Fig. 7(b). The same part is then considered with a slight taper along one of the axial directions next, and as shown in Fig. 8, tapered curved layers and deposition path patterns are successfully developed without any defects.

The simple curved part is then considered with a through hole at the top to test the ability to process thin shell like components with some internal details. While the basic shape of the CAD model is as shown in Fig. 9(a), a complication arises in that the continuous paths would lead to errors in obtaining the hole in the printed part. A modification was necessary, to develop the deposition pathways generated for the portions of the part on either side of the hole. The two parts, however, get connected through one extra line, as seen in Fig. 9(b), and this problem could not be completely resolved in the current modeling procedure. A manual elimination is easy, but a temporary stopping of the flow of the deposition material or subsequent trimming is attempted currently. Otherwise, the algorithm worked well and the curved layers and deposition path patterns built for this case are as shown in Fig. 9(b).

6. Implementation for curved layer printing

Test beds of varying capabilities are usually developed by researchers to test modified approaches in RP, and the Fab@Home FDM machine developed by Evan Malone of Cornell University (Fab@Home, 2010) is employed in the current research for the initial testing of the mathematical algorithms developed for CLFDM.

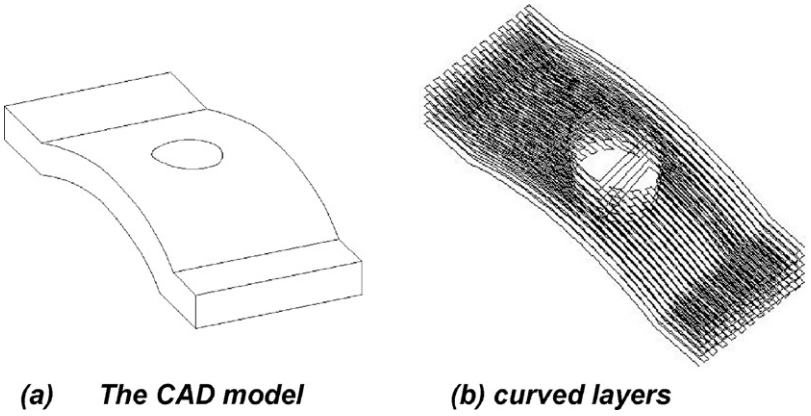

Fig. 9. A thin and curved part with a through hole. (a) The CAD model; (b) curved layers.

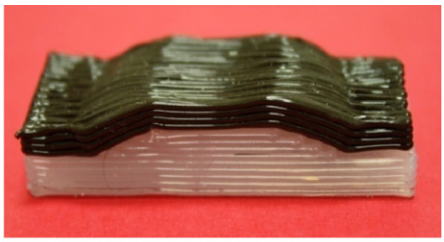

(a) Simple curved layer part

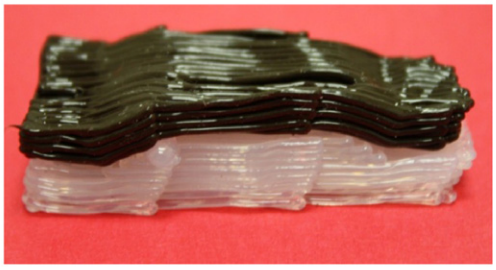

(b) The tapered curved layer part

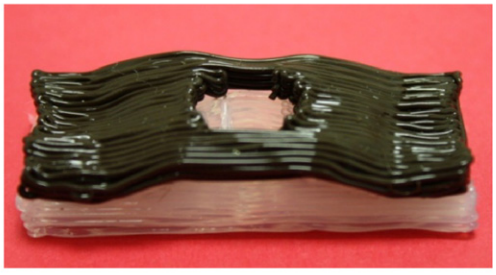

(c) The simple curved part with a central hole

Fig. 10. Curved layer parts together with the support structure printed using Silicone.

This has a standard syringe type deposition tool which consists of a disposable syringe. This system is adopted for the physical implementation of the curved layer models developed here and the output from the MATLAB code is a text file that contains deposition path data to control the machine for printing various models in curved layers.

For initial trials and proof of concept, SILAFLEX RTV Silicone, which is a room temperature vulcanising silicone household sealant available in several colours, is employed as the fused material. It is easily dispensed from a variety of taper tip diameters, tolerates high temperatures (200 °C), and is chemically very inert. It is tack free in 1–2 h per mm of thickness, and fully cured in 24 h into a semi-soft rubber material. Though it works perfectly for a physical implementation of the current models, the parts however, are rubber-like and cannot be tested for mechanical properties.

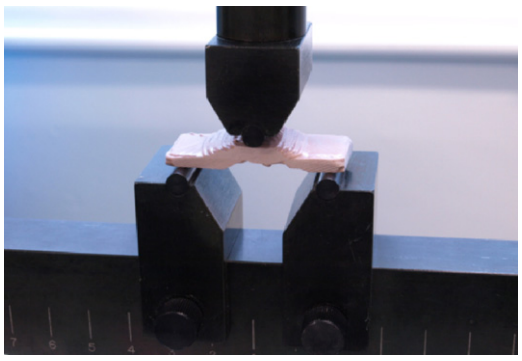

Fig. 12. A test part loaded for 3-point bending test.

The three test parts printed using silicone along with the support structures are shown in Fig. 10. Essentially, in each case, the starting point is the CAD model of the component, followed by the surface point data evaluation through G and M codes, and subsequent processing by the modified vector curved layer slicing algorithm in MATLAB for five consecutive layers. Text files containing support structure data as well as the curved layer data are loaded on the printer one after the other, and printed as shown in Fig. 10 using silicone of two different colours for the sake of clarity. It is evident that the parts, though following the required deposition pattern as per the outcomes of the CLFDM scheme, suffer from defects due to either the absence of a certain strand or the overriding of the nozzle. These are practical limitations of the test bed with limited control over the material flow, and it was very difficult to ensure the continuous flow of the material.

7. Testing

The next step is to print parts using both flat and curved layer FDM for a comparative analysis of mechanical performance. FabEpoxy (2010), a special 2 part epoxy formulated for Fab@Home by Kraftmark Company of Spring City, PA, USA, designed to be thixotropic, meaning that it will flow when it is extruded, but does not flow after extrusion is tried initially for testing the mechanical characteristics of parts produced. It was much easier to work with Fabepoxy, as it had better extrusion as well as post extrusion characteristics. This may be evident in the simple curved object printed using both flat and curved layers as shown in Fig. 11(a) and (b), respectively. A three point bending test conducted with the specimens loaded as shown in Fig. 12 revealed that the curved layer part fails at 152 N, as against the maximum load of 70 N supported by the flat layered part.

(a) Flat layered (b) Curved layered

Fig. 11. Parts printed using Fabepoxy. (a) Flat layered; (b) curved layered.

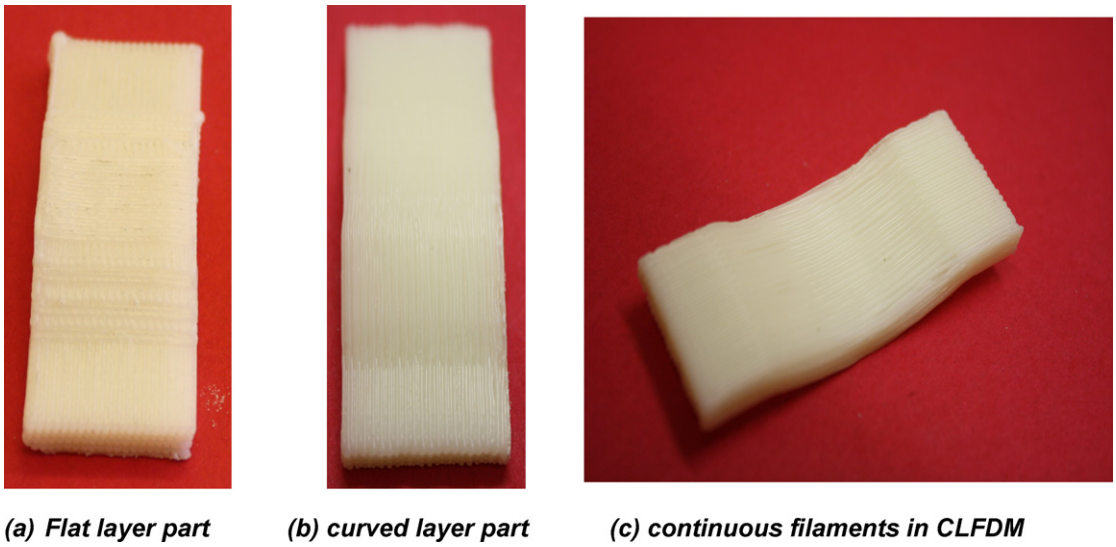

Fig. 13. Flat and curved parts printed using ABS polymer. (a) Flat layer part; (b) curved layer part; (c) continuous filaments in CLFDM.

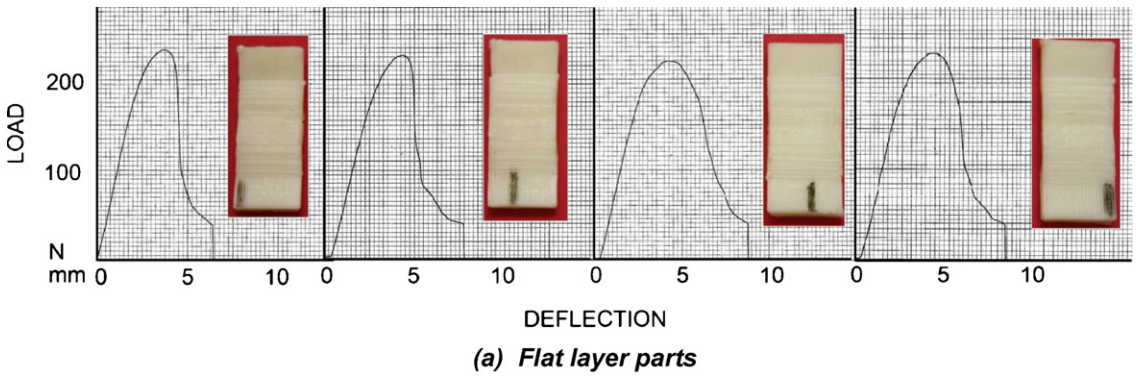

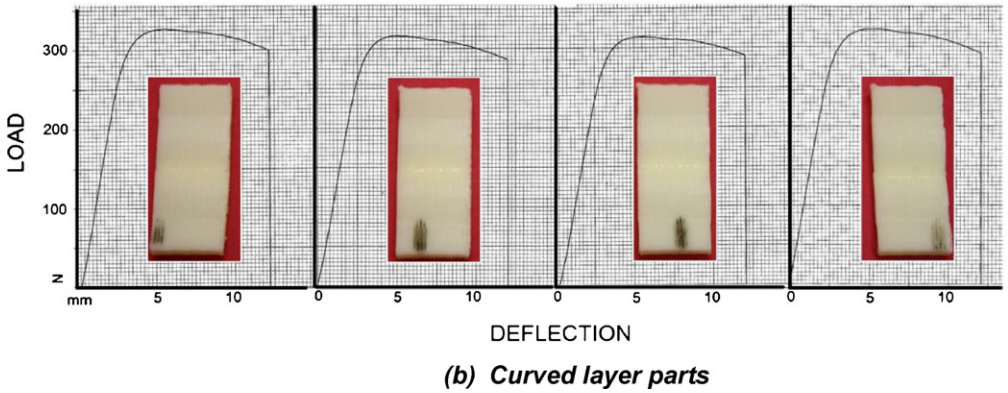

Fig. 14. Load deflection diagrams from tensile tests. (a) Flat layer parts; (b) curved layer parts.

Table 1
Results of 3-point bending tests.

Build style	Maximum compressive load (*N*)					
	Part 1	Part 2	Part 3	Part 4	Average	Standard deviation
Flat layer	220.000	233.666	227.000	228.333	227.2498	5.63
Curved layer	326.666	316.666	314.000	322.666	319.9995	5.73

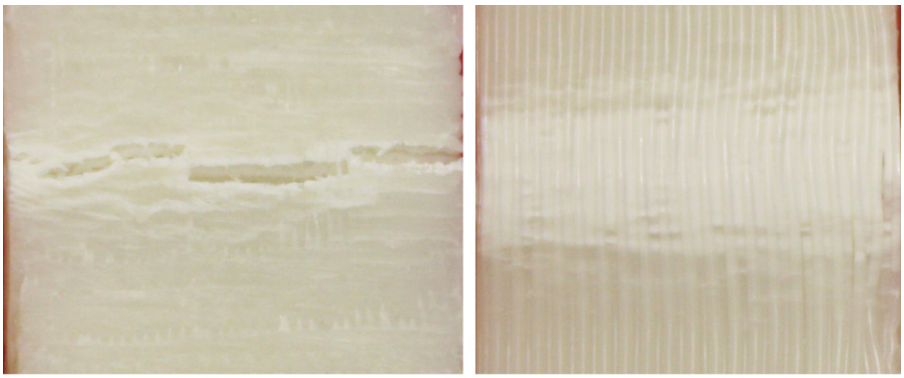

Fig. 15. Close-up views of deformation patterns. (a) Flat layer FDM; (b) curved layer FDM.

The curved part remained mostly intact until the end of the failure, which was a sudden fracture from the bottom upwards, almost at the middle of the length of the part. The continuous fibres fused together very well, reducing the gap structure, and the cured polymer seemed to have formed a well integrated molecular structure across the filaments as well as layers. The flat layered part on the other hand, gradually gave in at almost half the load, due to a shear slip across the layers. Failure seemed to have initiated at the junction of the curved and flat portions of the part, where there was possible stress concentration, and finally the weak interlayer bonds gave away for a shear failure, allowing successive flat layers to slide against one another.

While the improvement in mechanical performance of the part produced by CLFDM almost by 100% is very encouraging, it is early to conclude based on results obtained from just a couple of test pieces. A statistical validation of these results is essential and further, a real engineering material needs to be considered to test the concept close to the reality. Further experimental investigations are planned and conducted based on a different test platform this time, the Makerbot (Makerbot.com, 2011). The kit was bought and assembled and necessary changes were made to the MATLAB code to build part files suitable for processing on this new setup. Another advantage is that the test material in this case is ABS polymer, which is the most common material for FDM and has engineering significance.

The actual test consists of printing four samples each of the same basic shape as earlier, using both flat and curved layer FDM. The flat and curved parts printed are shown in Fig. 13(a) and (b), respectively and the surface quality is distinctly better in CLFDM. A view of the back side of the CLFDM part as shown in Fig. 13(c) clearly shows the continuous filaments stacked parallel to one another. Fig. 14(a) and (b) presents scanned copies of the load–deflection diagrams obtained from the 3-point bending tests performed on the two sets of samples together with photographs of deformed samples. The experimental data in terms of the maximum compressive load in each case is compiled in Table 1 for a statistical evaluation of the comparative performance of flat and curved layer FDM. The average compressive load in the case of flat layered components falls short by almost about 100 N compared to the curved layer parts, clearly indicating a much better mechanical performance by CLFDM. The standard deviation in both cases is relatively small and very close, indicating consistency and the experimental error with a 95% confidence level is approximately ±11 N.

Fig. 15(a) and (b) shows the bottom surfaces of the compressed flat and curved layer specimens respectively close to the deformation and fracture zones. It is evident that all the flat layer parts are severely stressed and cracked almost uniformly at the central zones of the bottom layers, while the curved parts seem to have only undergone some stretching and local distortion, with the continuous filament structure still intact. A closer look at the critical zones of deformation in both cases as shown in Fig. 15(a) and (b) reveals initiation of cracks at the bottom most layers and subsequent growth across the width in the case of the flat layered components. Possible reason for this could be the stress concentration on the ill formed filament structure leading to a snapping of individual strands and subsequent gross failure due to the propagation of the shearing action across layers. The same action on the curved parts could only result in a localised distortion as a number of parallel filaments, sufficiently fused into one another act together to resist deformation and crack formation.

8. Conclusion

Algorithms for curved layer slicing are developed based on practical solutions. Application of the algorithms in different cases of varying geometrical complexity proved the models to be effective. CLFDM is successfully implemented and physical parts are generated using both fabepoxy and ABS polymer. Experimental results indicate better mechanical performance by parts produced using curved layer FDM. The average fracture compressive load of curved layer parts under three point bending increased almost by 40% compared to that of the flat layer counter parts. While this could be attributed to the improved mesostructure, fracture zones clearly indicated improved structural integrity due to continuous fibres resulting from CLFDM.

References

Agarwala, M.K., Jamalabad, V.R., Langrana, N.A., Safari, A., Whalen, P.J., Danforth, S.C., 1996. Structural quality of parts processed by fused deposition. Rapid Prototyping Journal 2, 4–19.

Allahverdi, M., Danforth, S.C., Jafari, M., Safari, A., 2001. Processing of advanced electroceramic components by fused deposition technique. Journal of the European Ceramic Society 21, 1485–1490.

Anitha, R., Arunachalam, S., Radhakrishnan, P., 2001. Critical parameters influencing the quality of prototypes in fused deposition modeling. Journal of Material Processing Technology 118, 385–388.

Bellehumeur, C., Li, L., Sun, Q., Gu, P., 2004. Modelling of bond formation between polymer filaments in the fused deposition modelling process. Journal of Manufacturing Processes 6 (2), 170–178.

Chakraborty, D., Reddy, B.A., Roy Choudhury, A., 2008. Extruder path generation for curved layer fused deposition modeling. Computer Aided Design 40, 235–243.

Diegel, O., Singamneni, S., Huang, B., Gibson, I., 2011a. Curved layer fused deposition modeling in conductive polymer additive manufacturing. Advanced Materials Research 199–200, 1984–1987.

Diegel, O., Singamneni, S., Huang, B., Gibson, I., 2011b. Getting rid of wire: curved layer fused deposition modeling in conductive polymer additive manufacturing. Key Engineering Materials 467–469, 662–667.
Fab@Home, 2010. http://www.fabathome.org/wiki/index.php?title=Main_Page.
FabEpoxy, 2010. http://www.kraftmark.biz/pdfs/Fabepoxy/FabEpoxy.infosheet.pdf.
Harlev, 2005. http://www.mathworks.com/matlabcentral/fileexchange/6678-stlread.
Hope, R.L., Roth, R.N., Jacobs, P.A., 1997. Adaptive slicing with sloping layer surfaces. Rapid Prototyping Journal 3, 89–98.
http://wiki.makerbot.com/cupcake, 2011.
Hu, Z., Lee, K., Hur, J., 2002. Determination of optimal build orientation for hybrid rapid-prototyping. Journal of Material Processing Technology 130–131, 378–383.
Jamieson, R., Hacker, H., 1995. Direct slicing of CAD models for rapid prototyping. Rapid Prototyping Journal 1.
Klosterman, D.A., Chartoff, R.P., Osborne, N.R., Graves, G.A., Lightman, A., Han, G., Bezeredi, A., Rodrigues, S., 1999. Development of a curved layer LOM process for monolithic ceramics and ceramic matrix composites. Rapid Prototyping Journal 5, 61–71.
Kulkarni, P., Dutta, D., 1996. An accurate slicing procedure for layered manufacturing. Computer Aided Design 28, 683–697.
Lee, C.S., Kim, S.G., Kim, H.J., Ahn, S.H., 2007. Measurement of anisotropic compressive strength of rapid prototyping parts. Journal of Material Processing Technology 187–188, 627–630.
Luo, R.C., Yu, P.T., Lin, Y.F., Leong, H.T., 1999. Efficient 3D CAD model slicing for rapid prototyping manufacturing system. In: IECON '99 Proceedings, The 25th Annual Conference of the IEEE, vol. 3, pp. 1504–1509.
Rodriguez, J.F., Thomas, J.P., Renaud, J.E., 2000. Characterisation of the mesostructure of fused deposition acrylonitrile butadiene–styrene materials. Rapid Prototyping Journal 6 (3), 176–185.
Rodriguez, J.F., Thomas, J.P., Renaud, E.J., 2001. Mechanical behaviour of acrylonitrile butadiene styrene (ABS) fused deposition materials, experimental investigation. Rapid Prototyping Journal 7 (3), 148–158.
Sabourin, E., Houser, S.A., Bohn, J.H., 1996. Adaptive slicing using stepwise uniform refinement. Rapid Prototyping Journal 2, 20–26.
Xu, F., Loh, H.T., Wong, Y.S., 1999. Considerations and selection of optimal orientation for different rapid prototyping system. Rapid Prototyping Journal 5, 54–56.
Yang, Y., Fuh, J.Y.H., Loh, H.T., Wang, Y.G., 2002. Equidistant path generation for improving scanning efficiency in layered manufacturing. Rapid Prototyping Journal 8, 30–37.